Performance Evaluation of NARX-CG Model for Electricity Forecasting: Bali Blackout Case Study

Tengku Reza Suka Alaqsa*, Zulfatri Aini

Department of Electrical Engineering, Faculty of Science and Technology, Universitas Islam Negeri Sultan Syarif Kasim
H.R. Soebrantas Street, KM.15, Pekanbaru, 28293, Indonesia
**Corresponding author: tengku.reza2002@gmail.com*

Abstract— Bali experienced a widespread blackout in May 2025 that disrupted economic and social activities across the island, revealing weaknesses in electricity demand forecasting and system resilience. This study evaluates the performance of a Hybrid Nonlinear Autoregressive with Exogenous Inputs-Conjugate Gradient (NARX-CG) model as an advanced electricity forecast. The dataset covers the 2018-2023 period and includes six variables: electricity energy, connected capacity, number of customers, tariffs, Gross Regional Domestic Product (GRDP), and population, aligned with the national electricity planning framework. The NARX-CG model was developed using a 6-12-6-1 network architecture and trained with tansig transfer function. Forecasting performance was evaluated using Mean Squared Error (MSE) and Mean Absolute Percentage Error (MAPE) metrics. Results show that the NARX-CG model achieved an MSE of 0.09853 and an average MAPE of 8.12%, outperforming conventional projections with a MAPE of 28.48%. Yearly evaluations show consistent model stability, with the lowest MAPE values of 1.93% and 5.86% in 2023 and 2022, respectively. The NARX-CG model effectively captures nonlinear temporal dependencies, enhances predictive accuracy, and contributes to improved power system reliability and resilience, providing valuable insights for adaptive energy planning following the 2025 Bali blackout.

Keywords— Bali blackout; conjugate gradient; forecasting; NARX; performance evaluation

I. INTRODUCTION

Bali was plunged into darkness in early May 2025 when a widespread blackout halted activities across the island, disrupting one of the world's most prominent tourist destinations [1]. The blackout began on May 2, 2025, and quickly spread on X social media under the hashtag "*Bali Blackout*" as the crisis gained nationwide attention [2]. Government authorities confirmed that the outage stemmed from disturbances in the undersea transmission cable linking Java and Bali, which caused a total shutdown lasting until the evening [3]. Although the primary trigger was a technical failure in the transmission infrastructure, the severity and duration of the blackout raised concerns regarding the adequacy of system reserves and operational preparedness. This condition is closely linked to electricity demand forecasting accuracy, because inaccurate projections can lead to insufficient reserve margins, inappropriate generation scheduling, and poor contingency planning, thereby amplifying the impact of technical faults that would otherwise be manageable. Therefore, questions remain as to whether forecasting weaknesses contributed to the scale of the disruption, particularly as the National Electricity Utility (PLN) prepares long-term supply plans using the Rencana Usaha Penyediaan Tenaga Listrik (RUPTL) document [4]. However, the forecasting approach within RUPTL still relies heavily on linear regression, which is increasingly inadequate to capture the complexities and dynamics of modern energy demand [5].

Although RUPTL serves as the central guideline for electricity system planning, significant forecast errors have been observed in practice. For example, in North Sumatra Province, forecast errors in electricity consumption consistently exceeded 10% between 2018 and 2023. In 2018, actual consumption reached 10,445.02 GWh compared to the forecasted 11,500 GWh, resulting in a 10.10% error [4], [6]. The following year, the error rose to 11.95%, with actual consumption at 10,943.86 GWh and a forecast of 12,252 GWh [4], [7]. By 2020, forecast inaccuracies escalated to 21.45%, where actual usage stood at 11,192.85 GWh compared to the forecast of 13,594 GWh [4], [8]. The trend persisted into 2021 with an error of 25.38% [4], [9], followed by 31.59% in 2022 [4], [10], and peaked in 2023 with an error of 36.92%, where actual demand was 12,472.84 GWh against the forecast of 17,078 GWh [4], [11]. These consistent deviations highlight the limitations of existing methods.

Comparable inaccuracies have also been recorded in Java, particularly within DKI Jakarta, where forecast errors similarly exceeded 10% during the 2018-2023 period. In 2018, the actual demand was 32,779.20 GWh, while the forecast projected 36,444 GWh, producing an error of 11.18% [4], [6]. By 2019, the discrepancy increased to 11.74%, with actual consumption of 34,107.98 GWh compared to the forecasted 38,111 GWh [4], [7]. The gap widened further in 2020, with a 23.80% error [4], [8], followed by 28.01% in 2021 [4], [9]. Although the percentage slightly declined to 27.25% in 2022, accuracy remained insufficient [4], [10]. In 2023, the error was still high at 24.87%, with actual demand of 36,992.35 GWh against a forecast of 46,194 GWh [4], [11]. Similar or higher errors were also found in West Kalimantan, where deviations consistently exceeded 30% across the period [4]-[11], and in South Sulawesi, where errors surpassed 16% annually, with peaks of 31.56% in 2020 [4], [8].

These national-scale forecast deviations are relevant to the Bali because RUPTL adopts a unified planning methodology

Received 29 October 2025, Revised 5 December 2025, Accepted 9 December 2025.
DOI: https://doi.org/10.15294/jte.v17i2.35519

that applies the same forecasting framework across all regional systems [4]-[8]. Thus, the persistent errors observed in multiple provinces reflect systemic weaknesses in the national forecasting model rather than isolated regional failures. Since Bali's electricity demand planning and reserve margin allocation are also based on RUPTL projections, similar inaccuracies may occur within the Bali system and could weaken operational resilience when facing unexpected disturbances such as the May 2025 blackout. Therefore, evaluating forecasting performance in Bali becomes critical to preventing the amplification of technical failures through inadequate demand prediction and reserve planning.

As technology advances, neural networks have emerged as a superior alternative for data analysis and forecasting because of their ability to mimic the structure and function of the human brain [12]. Neural networks consist of layers of interconnected artificial neurons, where each neuron processes and transmits information [13]. Among various neural network methods, the nonlinear autoregressive model with exogenous inputs (NARX) has demonstrated particularly strong forecasting performance. For instance, studies reported mean square error (MSE) values as low as 0.0521, 0.0040, and 0.0006 in solar radiation prediction [14]. In photovoltaic power output forecasting, the normalized root mean square error (nRMSE) reached just 1.98% [15]. Furthermore, NARX achieved a performance accuracy of 94% in predicting wind speed for wind energy generation [16], while another study reported an MSE of 0.0666 in wind speed forecasting applications [17].

The strength of the NARX model lies in its role as a dynamic surrogate model designed to approximate complex system behavior and capture temporal dependencies within real systems. In many engineering applications including power system stability forecasting, the future value of a variable cannot be determined solely from its present state but is influenced by historical patterns and external disturbances [18]. A deterministic system evolves over time, where the future output $y(t+1)$ depends not only on past outputs $y(t), y(t-1), \dots, y(t-n_y+1)$ but also on lagged external inputs $u(t), u(t-1), \dots, u(t-n_u+1)$ [19]. This algorithm NARX to predict $y(t+1)$ by combining autoregressive terms with delayed exogenous variables, while accounting for a stochastic residual component $e(t)$ [20]. The regressor vector $\Phi(t)$ is constructed by stacking these delayed endogenous and exogenous terms, forming a design matrix Ψ that represents the system's dependencies [21]. Unlike traditional linear regression, where models often fail to capture nonlinear dynamics, this structure provides flexibility to handle dynamic systems even when data are limited or costly to obtain. Model parameters c are optimized by minimizing the discrepancy between observed values Y_{ED} and predicted responses $\Psi_{ED}c$, shows that the estimated coefficients represent the system as accurately as possible [22]. Given Bali's vulnerability to large-scale system disturbances, a forecasting model capable of responding to nonlinear and rapidly changing demand patterns is needed to enhance reserve allocation and operational decision-making. Therefore, the adoption of NARX is expected to provide more accurate demand predictions and strengthen system reliability, especially reducing the risk of widespread blackouts in the future.

In surrogate modeling, the coefficient vector c may represent weights in polynomials or neural networks, and its estimation can be carried out using least-squares minimization or regularization techniques. When the formulation is linear-in-parameters, coefficients can be obtained through analytical optimization methods, while more advanced approaches such as LASSO [23]. Although various neural network-based forecasting approaches such as Backpropagation, Recurrent Neural Networks have been widely applied in time-series prediction, their performance often declines when facing highly volatile demand patterns and complex nonlinear dependencies. In contrast, NARX explicitly incorporates historical demand $y(t)$ and delayed exogenous inputs $u(t)$, to capture nonlinear fluctuations more effectively and produce interpretable yet accurate forecasting results. The study aims to investigate additional factors influencing electricity demand and to demonstrate how accurate demand forecasting can be achieved using the NARX method optimized via the Conjugate Gradient algorithm. Forecasting results obtained with NARX are compared against those produced under PLN's RUPTL framework to evaluate the relative performance of both approaches.

II. Method

A. NARX Model Proposed Algorithm: Bali Blackout Case

Deterministic dynamical system M evolves along the time domain T. Its evolution is influenced by external signals $X_{Bali}(t) \in \mathbb{R}^6$, consisting of electricity energy, connected capacity, number of customers, electricity tariff, GRDP, and population. With an initial condition vector β, the corresponding system output, i.e., actual electricity consumption of Bali $Y_{Bali}(t) \in \mathbb{R}$, at each instant $t \in T$ is written as (1) [24].

$$Y_{Bali}(t) = M(X_{Bali}(T \leq t), \beta) \tag{1}$$

The notation $X_{Bali}(T \leq t)$ highlights that the outcome at time t reflects the influence of all six input variables up to that moment. For clarity, the term β is omitted unless explicitly required. An approximate representation of the true dynamics can be introduced through a surrogate model $\widehat{M}$, written as (2) [25].

$$\hat{Y}_{Bali}(t) = \widehat{M}(X_{Bali}(T \leq t), \beta) \approx M(X_{Bali}(T \leq t), \beta) \tag{2}$$

Such a surrogate is often built using nonlinear autoregressive models with exogenous inputs (NARX). Within this framework, the system behavior is described at discrete time instants $\{0, \delta t, \dots, (N-1)\delta t\}$, and the upcoming response of Bali's electricity consumption is approximated using a combination of past outputs and external inputs, written as (3) [24].

$$\hat{Y}_{Bali}(t+\delta t) = \widehat{M}(X_{Bali}(T \leq t + \delta t), Y_{Bali}(T < t + \delta t); c) + \varepsilon(t) \tag{3}$$

where $\varepsilon(t) \sim N(0, \sigma_\varepsilon)$ denotes a zero-mean residual with variance σ_ε. The mapping $\widehat{M}$ is assumed to be parametric and defined by a finite parameter vector c. Training this model requires estimating c from a collection of input-output trajectories $(X_{Bali}^{(i)}, Y_{Bali}^{(i)})$, called realizations. The entire collection is referred to as the experimental design (ED), shown in (4) [24].

$$D = \{(X_{Bali}^{(i)}, Y_{Bali}^{(i)}),\ X_{Bali}^{(i)} \in \mathbb{R}^{N \times 6},\ Y_{Bali}^{(i)} = M(X_{Bali}^{(i)}) \in \mathbb{R}^N,\ i = 1, \dots, N_{ED}\} \tag{4}$$

The size of the experimental design is usually modest, because obtaining each realization may involve costly simulation or experimentation. Equation (3) can be restated in a more explicit form as (5) [24].

$$\hat{Y}_{Bali}(t+\delta t) = \hat{M}(\phi_{Bali}(t+\delta t); c), \quad \phi_{Bali}(t) \in \mathbb{R}^n \tag{5}$$

where the regressor vector $\phi_{Bali}(t)$ is given by (6) [26]:

$$\phi_{Bali}(t) = \{Y_{Bali}(t-\delta t), \dots, Y_{Bali}(t - n_y\delta t), X_1(t), X_1(t-\delta t), \dots, X_6(t-n_{x_6}\delta t)\} \tag{6}$$

with X_1 = electricity energy, X_2 = connected capacity, X_3 = number of customers, X_4 = electricity tariff, X_5 = GRDP, and X_6 = population. By collecting all regressor vectors $\phi_{Bali}(t)$ across time steps, the design matrix $\Phi_{Bali} \in \mathbb{R}^{N\times n}$ is formed. The outputs are arranged into vector $Y_{Bali} \in \mathbb{R}^{\bar{N}}$, written as (7) [24].

$$\Phi_{Bali} = \begin{bmatrix} \phi_{Bali}(t_0) \\ \phi_{Bali}(t_0+\delta t) \\ \vdots \\ \phi_{Bali}((N-1)\delta t) \end{bmatrix}$$

$$Y_{Bali} = \begin{bmatrix} Y_{Bali}(t_0) \\ Y_{Bali}(t_0+\delta t) \\ \vdots \\ Y_{Bali}((N-1)\delta t) \end{bmatrix} \tag{7}$$

Even though the dataset originates from time-series observations, the pairs $\{\phi_{Bali}(t), Y_{Bali}(t)\}$ do not necessarily need to preserve temporal order. Consequently, for $i = 1, \dots, N_{ED}$, the matrices $\Phi_{Bali}^{(i)}$ and vectors $Y_{Bali}^{(i)}$ can be combined to construct (8) [24].

$$\Phi_{ED} = \begin{bmatrix} \Phi_{Bali}^{(1)} \\ \vdots \\ \Phi_{Bali}^{(N_{ED})} \end{bmatrix} \quad Y_{ED} = \begin{bmatrix} Y_{Bali}^{(1)} \\ \vdots \\ Y_{Bali}^{(N_{ED})} \end{bmatrix} \tag{8}$$

The goal is to obtain a predictive model $\hat{M}$ described by parameters c, estimated solely from the available ED. The parameter vector is identified by minimizing a loss function L, which quantifies the mismatch between observed outputs and predicted responses, as (9) [24].

$$\hat{c} = \underset{c}{\operatorname{argmin}}\ L(Y_{ED}, \hat{M}(\Phi_{ED}; c)) \tag{9}$$

A common set of surrogate models $\hat{M}$ involves the use of neural networks, where the parameter vector c contains the weights and biases. Among these, models expressed in a linear form with respect to their parameters are often emphasized, since the optimization reduces to least-squares as (10) [24].

$$\hat{c} = \underset{c}{\operatorname{argmin}}\ \| Y_{ED} - G(\Phi_{ED})c \|_2^2 \tag{10}$$

With the definition $\Psi_{ED} = G(\Phi_{ED})$, the parameter vector c can be obtained analytically through ordinary least squares (OLS), written as (11) [24].

$$\hat{c} = (\Psi_{ED}^\top \Psi_{ED})^{-1}\Psi_{ED}^\top Y_{ED} \tag{11}$$

Enhanced regression schemes such as LASSO can be used, which introduce an l^1-norm penalty alongside a regularization factor γ, shown in (12) [24].

$$\hat{c} = \underset{c}{\operatorname{argmin}}\ \| Y_{ED} - \Psi_{ED}c \|_2^2 + \gamma \| c \|_1 \tag{12}$$

This study applies conjugate gradient (CG) optimization to adjust step size without requiring second-order derivatives, reducing computational cost. The CG update is implemented as (13)-(14) [27].

$$Y_{Bali}^{(i+1)} = v^{(i+1)} + Y_{Bali}^{(i)} + c^{(i)} \tag{13}$$

$$w^{(i+1)} = w^{(i)} + Y_{Bali}^{(i)}\eta^{(i)} \tag{14}$$

where the training direction at iteration $(i+1)$, denoted as $Y_{Bali}^{(i+1)}$, is computed by summing the current gradient $v^{(i+1)}$, the previous direction $Y_{Bali}^{(i)}$, and the conjugate parameter $c^{(i)}$. The parameter update is given by the weights $w^{(i)}$ and $w^{(i+1)}$, while $\eta^{(i)}$ is the learning rate.

B. Dataset

The dataset used in this study includes secondary data collected from various official sources covering the period from 2018 to 2023 in Bali Province. The six-year range is selected because consistent and category-matched data for all required variables are only available for this period. Earlier datasets do not contain complete or uniform records across all forecasting parameters, which is unsuitable for developing a comparable multivariate forecasting model. Since time-series forecasting requires data with consistent structure and synchronized variables, using incomplete or mismatched categories would introduce bias and reduce model reliability. Therefore, the 2018-2023 dataset represents the most valid and methodologically feasible time window for analysis.

The variables are electricity energy (GWh), connected capacity (MVA), number of customers, electricity tariff (Rp/kWh), Gross Regional Domestic Product (GRDP in billion Rp), and population (persons). These align with the variables used in PLN's Rencana Usaha Penyediaan Tenaga Listrik (RUPTL) [2], [6]-[11].

The electricity tariff varied, ranging from Rp 877.83/kWh in 2018 to Rp 1,333.12/kWh in 2023. There were significant increases in 2019 and 2022 that may have affected consumption behavior. The Gross Regional Domestic Product (GRDP) showed dynamic trends, rising from Rp 233,636.77 billion in 2018 to Rp 274,358.18 billion in 2023. The population gradually increased from 4,309,200 persons in 2018 to 4,404,260 persons in 2023. Figure 1. shows input data in this research.

The target data for model training represents actual electricity energy consumption in Bali Province for 2018-2023 and corresponds with the input variables mentioned above [6]-[11], [28], [29]. To validate comparisons, RUPTL projection data were used as reference targets [4].

C. Performance Evaluation

The network is configured with six input variables, structured as a 6-12-6-1 network. The selection of this configuration is based on the *2N* heuristic rule, where *N* represents the number of input neurons. With six input variables (*N* = 6), the recommended number of neurons in the hidden layer ranges around *2N* = 12, which provides an optimal balance between learning capacity and model generalization. Prior studies have demonstrated that applying the *2N* rule produces improved convergence and minimizes underfitting and overfitting in forecasting applications, particularly within nonlinear multivariate datasets [33]. The

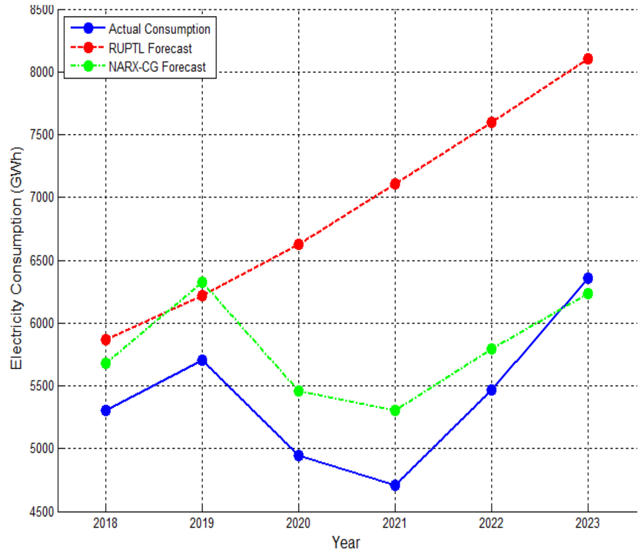

Figure 1. Comparison Actual Data, RUPTL, and NARX Conjugate Gradient

dataset is simulated and processed in MATLAB. Prior to training, the input data are normalized to the range (-1, 1) using the hyperbolic tangent sigmoid (*tansig*) transfer function, as expressed in (15) [31].

$$Xn = 2 \,.\, \frac{Xp - \min\,(Xp)}{\max\,(Xp) - \min\,(Xp)} - 1 \tag{15}$$

The forecasting simulation output will be evaluated using MSE, as expressed in (16) [31].

$$MSE = \frac{1}{n} \sum_{t=1}^{n} (Y_i - \hat{y}_t)^2 \tag{16}$$

where, MSE is the Mean Square Error, n is the number of data points, Y_i is the actual data, and $\hat{y}_t$ is the forecasted data.

The data is denormalized to return it to the actual values using (17) [32].

$$X = 0.5\,.\,(Xn + 1).\,(\max(Xp)) - \min\,(Xp)) + \min\,(Xp)$$

where X represents the real data that has been denormalized, and Xn is the normalized data. The maximum value of the original real data is denoted as max{Xp}, while the minimum value is represented by min{Xp}

Then, the MAPE between the NARX-CG algorithm and the RUPTL is calculated for comparison using (18) [33].

$$MAPE = \frac{1}{n} \sum_{t=1}^{n} \left| \frac{Yt - \dot{Y}t}{Yt} \right| .\, 100\% \tag{18}$$

where n represents the total number of data points, Yt denotes the actual data values, and $\dot{Y}t$ signifies the forecasted values.

III. Results and Discussion

The simulation was performed using the NARX Conjugate Gradient model based on (1)-(15). The Mean Squared Error (MSE) for Bali Province was calculated using (16), as shows in Table I. The output data of the NARX Conjugate Gradient network were denormalized to obtain the predicted electricity consumption in actual units (GWh) using (17). The denormalized output was then used to calculate the Mean Absolute Percentage Error (MAPE) for the NARX-CG according (18). The results in Table I shows that the NARX Conjugate Gradient model provides varying degrees of accuracy across the 2018-2023.

To evaluate the relative performance, the MAPE of the NARX-CG forecasts was compared with the MAPE of PLN's RUPTL projections, which are based on the same input variables. The comparison allows for assessing which method provides more accurate electricity consumption forecasting. The results are presented in Table II.

The MSE for the model is calculated as 0.09853, shows generally small discrepancy between the normalized target data and the network output. Specifically, years such as 2018, 2020, 2021, and 2022 shows negligible squared errors. The largest deviation occurs in 2019, where the squared error reaches 0.53684, shows that the model experienced a transient difficulty capturing extreme fluctuations in the target signal. This anomaly is associated with significant disruptions in national and regional economic performance leading up to the COVID-19 pandemic, which began impacting Indonesia at the end of 2019 and escalated in early 2020. The pre-pandemic slowdown triggered irregular patterns in electricity demand due to reduced industrial operations, shifts in business activities, and early contraction across tourism-dependent regions such as Bali. Consequently, the instability in consumption patterns during this transitional period introduced high variability in the time-series signal, making it more challenging for the NARX model to learn consistent temporal relationships, where the output at each time step is influenced by past inputs and outputs through the regressor vector Φ(t) [24].

Table II shows the denormalized output of NARX-CG alongside the RUPTL forecasts and actual electricity consumption. The average MAPE of NARX-CG is 8.12%, significantly lower than the 28.48% observed in RUPTL forecasts. This discrepancy highlights the good performance of the NARX-CG model in capturing the nonlinear and dynamic behavior of electricity demand in Bali Province. Notably, in years such as 2022 and 2023, NARX-CG achieves MAPE values of 5.86% and 1.93%, respectively, shows robust predictive capabilities even in periods with rapidly increasing consumption. The comparison show the limitations of the RUPTL method, which relies primarily on linear regression and fails to capture complex demand dynamics. Consequently, NARX-CG emerges as a promising approach for more reliable short-and medium-term load forecasting.

TABLE I. MSE NARX Conjugate Gradient Bali Province

Year	Target	Output	Error	Squared Error
2018	-0.277680	-0.277620	0.000060	0.000000003600
2019	0.213110	0.945800	0.732690	0.536840000000
2020	-0.709880	-0.709940	-0.000060	0.000000003600
2021	-1.000000	-0.999600	0.000400	0.000000160000
2022	-0.073811	-0.073796	0.000015	0.000000000225
2023	1.000000	0.766950	-0.233050	0.054340000000
		MSE		**0.098530000000**

TABLE II. COMPARISON MAPE RUPTL AND NARX CONJUGATE GRADIENT BALI PROVINCE

Year	Actual Consumption Bali Province (GWh)	RUPTL Forecast (GWh)	NARX Conjugate Gradient Forecast (GWh)	MAPE RUPTL Forecast (%)	MAPE NARX CG Forecast (%)
2018	5,302.67	5,866	5682.6	10.62	7.16
2019	5,706.72	6,221	6326.0	9.01	10.87
2020	4,946.86	6,630	5455.2	34.02	10.31
2021	4,708.02	7,105	5302.9	50.91	12.61
2022	5,470.51	7,595	5789.8	38.84	5.86
2023	6,354.53	8,101	6232.0	27.48	1.93
MAPE				**28.48**	**8.12**

The errors observed in RUPTL forecasts, as evidenced by consistently high MAPE values, have practical consequences for electricity system reliability shows in Figure 1. Historical deviations exceeding 10% in multiple provinces, including Bali, suggest that RUPTL's linear assumptions fail to account for demand variability driven by population growth, economic activity, and seasonal patterns. The significant errors in years such as 2021 and 2022, where MAPE reaches 50.91% and 38.84%, respectively, shows potential risks in power planning. These inaccuracies may have contributed indirectly to system disturbances, such as the Bali blackout, by creating mismatches between supply and anticipated demand. By contrast, the lower MAPE achieved by NARX-CG shows that incorporating dynamic inputs and nonlinear modeling can reduce forecast errors and enhance operational planning.

The basis of the NARX model explains its improved performance relative to RUPTL. As a deterministic dynamic system, NARX incorporates both past outputs and delayed exogenous inputs to predict future electricity consumption, as shown in equations (1)-(12) [24]. The surrogate model $\widehat{M}$ approximates the true system dynamics by combining autoregressive lags with external drivers while accounting for stochastic residuals. By training the model on an experimental design (ED) comprising historical input-output trajectories, the parameter vector c is optimized to minimize forecast errors, as expressed in (9). The conjugate gradient algorithm further enhances optimization by efficiently updating network weights without requiring computationally expensive second-order derivatives. This combination of nonlinear regression and gradient-based optimization enables NARX-CG to handle temporal dependencies and capture fluctuations that traditional linear methods like RUPTL cannot.

Analyzing the year by year performance of NARX-CG by Figure 1. reveals that the model is particularly effective in stabilizing forecasts during periods of demand growth. For instance, while the MSE table shows large deviations in normalized 2021, the denormalized output achieves a forecast within 12.61% MAPE of actual consumption. In contrast, RUPTL projects consistently overestimate consumption, as seen in 2020 and 2021, in MAPE exceeding 30% and 50%, respectively. These observations are consistent with NARX theory, where the design matrix Φ and regressor vector $\varphi(t)$ capture both short-term fluctuations and long-term trends from past outputs and exogenous variables. Moreover, this result shows that the NARX-CG model maintains stability despite variations in data scaling, showing its robustness under fluctuating demand conditions. The ability of the model to preserve forecasting accuracy after denormalization suggests that the learned nonlinear relationships remain consistent across different data representations. Consequently, this characteristic supports the suitability of NARX-CG for long-term electricity demand analysis where structural changes and demand growth frequently occur.

IV. CONCLUSION

This study shows that the NARX Conjugate Gradient (NARX-CG) model provides strong performance in forecasting electricity consumption in Bali Province, achieving a MAPE of 8.12% and an MSE of 0.09853. By incorporating past outputs and delayed exogenous inputs, the model effectively captures nonlinear and time-dependent demand dynamics, as adaptive responses to consumption fluctuations and maintaining robust performance during periods of rapid growth. Furthermore, the inclusion of variables such as connected capacity, customer numbers, tariffs, GRDP, and population enhances the model's ability to represent complex demand behavior, supporting its applicability as a reliable tool for electricity planning. Future research may extend this work through comparative evaluations with advanced forecasting models such as LSTM and GRU, multi-step-ahead forecasting, real-time data integration from SCADA or smart meters, and the incorporation of probabilistic uncertainty analysis to support risk-based planning and reserve margin decision-making.

REFERENCES

[1] Bali Provincial Government, "Concerned about a Bali blackout, Minister of Environment and Forestry gives green light for the Sidakarya LNG Terminal," Bali Provincial Government, 2025. [Online]. Available: https://www.baliprov.go.id/web/khawatir-bali-blackout-menteri-lhk-beri-sinyal-hijau-untuk-terminal-lng-sidakarya/

[2] Y. C. A. Sanjaya, "Chronology of today's Bali blackout: Sudden power outage, coal-fired power plant suspected of disruption," KOMPAS.com, 2025. [Online]. Available: https://www.kompas.com/tren/read/2025/05/02/204500665/kronologi-bali-blackout-hari-ini--listrik-mendadak-padam-pltu-diduga?page=all

[3] M. A. Asnawi, "Bali in darkness, demanding the return of a clean energy transition," Mongabay.co.id, 2025. [Online]. Available: https://mongabay.co.id/2025/05/10/bali-gelap-menagih-kembali-transisi-energi-bersih/

[4] PT. PLN (Persero), *RUPTL PLN 2018-2027*, Jakarta: PT. PLN (Persero), 2018.

[5] S. Bansal and G. Singh, "Multiple linear regression based analysis of weather data: assumptions and limitations," in *International Conference on Advanced Communication and Intelligent Systems*, Cham: Springer Nature Switzerland, 2023, pp. 221-238.

[6] PT. PLN (Persero), *Statistic PLN 2018*, Jakarta: PT. PLN (Persero), 2018.

[7] PT. PLN (Persero), *Statistic PLN 2019*, Jakarta: PT. PLN (Persero), 2019.

[8] PT. PLN (Persero), *Statistic PLN 2020*, Jakarta: PT. PLN (Persero), 2020.

[9] PT. PLN (Persero), *Statistic PLN 2021*, Jakarta: PT. PLN (Persero), 2021.

[10] PT. PLN (Persero), *Statistic PLN 2022*, Jakarta: PT. PLN (Persero), 2022.

[11] PT. PLN (Persero), *Statistic PLN 2023*, Jakarta: PT. PLN (Persero), 2023.

[12] S. Zhu, T. Yu, T. Xu, H. Chen, S. Dustdar, S. Gigan, and Y. Pan, "Intelligent computing: the latest advances, challenges, and future," *Intelligent Computing*, vol. 2, 2023, Art. no. 0006.

[13] A. Thakur and A. Konde, "Fundamentals of neural networks," *International Journal for Research in Applied Science and Engineering Technology*, vol. 9, no. VIII, pp. 407-426, 2021.

[14] N. AL-Rousan and H. Al-Najjar, "A comparative assessment of time series forecasting using NARX and SARIMA to predict hourly, daily, and monthly global solar radiation based on short-term dataset," *Arabian Journal for Science and Engineering*, vol. 46, no. 9, pp. 8827-8848, 2021.

[15] M. Massaoudi, "An effective hybrid NARX-LSTM model for point and interval PV power forecasting," *IEEE Access*, vol. 9, pp. 36571-36588, 2021.

[16] R. S. Parente, D. Alencar, P. Junior, I. Silva, and J. Liete, "Application of the NARX model for forecasting wind speed for wind energy generation," *International Journal of Development Research*, vol. 11, no. 4, pp. 46461-46466, 2021.

[17] W. Masmoudi, A. Djebli, and F. Moussaoui, "Evaluating LSTM and NARX neural networks for wind speed forecasting and energy optimization in Tetouan, Northern Morocco," *Energy Exploration & Exploitation*, 2025, doi: 10.1177/01445987241309035.

[18] Y. Zhao, C. Jiang, M. A. Vega, M. D. Todd, and Z. Hu, "Surrogate modeling of nonlinear dynamic systems: a comparative study," *Journal of Computing and Information Science in Engineering*, vol. 23, no. 1, Art. no. 011001, 2023.

[19] L. F. B. Carbonera, D. Pinheiro Bernardon, D. de Castro Karnikowski, and F. Alberto Farret, "The nonlinear autoregressive network with exogenous inputs (NARX) neural network to damp power system oscillations," *International Transactions on Electrical Energy Systems*, vol. 31, no. 1, Art. no. e12538, 2021.

[20] A. H. Dhafer et al., "Empirical analysis for stock price prediction using NARX model with exogenous technical indicators," *Computational Intelligence and Neuroscience*, vol. 2022, Art. no. 9208640, 2022.

[21] W. M. Ashraf and V. Dua, "Partial derivative-based dynamic sensitivity analysis expression for nonlinear autoregressive with exogenous (NARX) model: case studies on distillation columns and model's interpretation investigation," *Chemical Engineering Journal Advances*, vol. 18, Art. no. 100605, 2024.

[22] K. Vidyalashmi et al., "Analysing the performance of the NARX model for forecasting the water level in the Chikugo River estuary, Japan," *Environmental Research*, vol. 251, Art. no. 118531, 2024.

[23] A. Kadochnikova, Y. Zhu, Z. Q. Lang, and V. Kadirkamanathan, "Integrated identification of the nonlinear autoregressive models with exogenous inputs (NARX) for engineering systems design," *IEEE Transactions on Control Systems Technology*, vol. 31, no. 1, pp. 394-401, 2022.

[24] S. Schär, S. Marelli, and B. Sudret, "Surrogate modeling with functional nonlinear autoregressive models (F-NARX)," *Reliability Engineering & System Safety*, 2025, Art. no. 111276.

[25] A. A. Joumah, A. Jafar, and C. Albitar, "Forward geometric model prediction of a 6-RSU parallel manipulator using a modified NARX Bayesian neural network," *Heliyon*, vol. 10, no. 24, 2024.

[26] H. Vu and D. Chang, "Optimising computational efficiency in dynamic modelling of proton exchange membrane fuel cell power systems using NARX network," *Energy Conversion and Management: X*, vol. 26, Art. no. 100908, 2025.

[27] N. A. Nasrudin, J. Jewaratnam, M. A. Hossain, and P. B. Ganeson, "Performance comparison of feedforward neural network training algorithms in modelling microwave pyrolysis of oil palm fibre for hydrogen and biochar production," *Asia-Pacific Journal of Chemical Engineering*, vol. 15, no. 1, Art. no. e2388, 2020.

[28] BPS Bali Province, *Bali Province GRDP at Current Prices by Expenditure*, Bali: Central Statistics Agency of Bali Province, 2025.

[29] BPS Bali Province, *Population Projection of Bali Province by Gender*, Bali: Central Statistics Agency of Bali Province, 2025.

[30] R. Sarkar, S. Julai, S. Hossain, W. T. Chong, and M. Rahman, "A comparative study of activation functions of NAR and NARX neural network for long-term wind speed forecasting in Malaysia," *Mathematical Problems in Engineering*, vol. 2019, Art. no. 6403081, 2019.

[31] S. Prayudani, A. Hizriadi, Y. Y. Lase, and Y. Fatmi, "Analysis accuracy of forecasting measurement technique on random K-nearest neighbor (RKNN) using MAPE and MSE," in *Journal of Physics: Conference Series*, vol. 1361, no. 1, p. 012089, IOP Publishing, 2019.

[32] Z. Liu, M. Cheng, Z. Li, Z. Huang, Q. Liu, Y. Xie, and E. Chen, "Adaptive normalization for non-stationary time series forecasting: A temporal slice perspective," *Advances in Neural Information Processing Systems*, vol. 36, pp. 14273-14292, 2023.

[33] Y. F. Utami, G. Darmawan, and R. S. Pontoh, "Forecasting Electricity Sales Using the Artificial Neural Network Backpropagation Method," *Asian Journal of Applied Education (AJAE)*, vol. 2, no. 4, pp. 581-594, 2023.